Platelets

ISSN: 0953-7104 (Print) 1369-1635 (Online) Journal homepage: http://www.tandfonline.com/loi/iplt20

# Inhibition of NMDA receptor function with an anti-GluN1-S2 antibody impairs human platelet function and thrombosis

Taryn N. Green, Justin R. Hamilton, Marie-Christine Morel-Kopp, Zhaohua Zheng, Ting-Yu T. Chen, James I. Hearn, Peng P. Sun, Jack U. Flanagan, Deborah Young, P. Alan Barber, Matthew J. During, Christopher M. Ward & Maggie L. Kalev-Zylinska

**To cite this article:** Taryn N. Green, Justin R. Hamilton, Marie-Christine Morel-Kopp, Zhaohua Zheng, Ting-Yu T. Chen, James I. Hearn, Peng P. Sun, Jack U. Flanagan, Deborah Young, P. Alan Barber, Matthew J. During, Christopher M. Ward & Maggie L. Kalev-Zylinska (2017): Inhibition of NMDA receptor function with an anti-GluN1-S2 antibody impairs human platelet function and thrombosis, Platelets, DOI: 10.1080/09537104.2017.1280149

**To link to this article:** http://dx.doi.org/10.1080/09537104.2017.1280149

platelets

http://www.tandfonline.com/iplt
ISSN: 0953-7104 (print), 1369-1635 (electronic)

Platelets, Early Online: 1–13
DOI: 10.1080/09537104.2017.1280149

Taylor & Francis
Taylor & Francis Group

ORIGINAL ARTICLE

# Inhibition of NMDA receptor function with an anti-GluN1-S2 antibody impairs human platelet function and thrombosis

Taryn N. Green[1], Justin R. Hamilton [2], Marie-Christine Morel-Kopp [3,4], Zhaohua Zheng[2], Ting-Yu T. Chen[1,5], James I. Hearn [1], Peng P. Sun[1], Jack U. Flanagan[6,7], Deborah Young [5], P. Alan Barber [8,9], Matthew J. During[1,10], Christopher M. Ward[3,4], & Maggie L. Kalev-Zylinska [1,11]

*[1]Department of Molecular Medicine and Pathology, University of Auckland, Auckland, New Zealand, [2]Australian Centre for Blood Diseases, Monash University, Melbourne, Australia, [3]Department of Haematology and Transfusion Medicine, Royal North Shore Hospital, Sydney, Australia, [4]Northern Blood Research Centre, Kolling Institute, University of Sydney, Sydney, Australia, [5]Department of Pharmacology and Clinical Pharmacology, University of Auckland, Auckland, New Zealand, [6]Auckland Cancer Society Research Centre, University of Auckland, Auckland, New Zealand, [7]Maurice Wilkins Centre for Molecular Biodiscovery, University of Auckland, Auckland, New Zealand, [8]Department of Neurology, Auckland City Hospital, Auckland, New Zealand, [9]Centre for Brain Research, University of Auckland, Auckland, New Zealand, [10]Departments of Molecular Virology, Immunology and Medical Genetics, Neuroscience and Neurological Surgery, Ohio State University, Columbus, OH, USA, and [11]LabPlus Haematology, Auckland City Hospital, Auckland, New Zealand*

## Abstract

GluN1 is a mandatory component of *N*-methyl-D-aspartate receptors (NMDARs) best known for their roles in the brain, but with increasing evidence for relevance in peripheral tissues, including platelets. Certain anti-GluN1 antibodies reduce brain infarcts in rodent models of ischaemic stroke. There is also evidence that human anti-GluN1 autoantibodies reduce neuronal damage in stroke patients, but the underlying mechanism is unclear. This study investigated whether anti-GluN1-mediated neuroprotection involves inhibition of platelet function. Four commercial anti-GluN1 antibodies were screened for their abilities to inhibit human platelet aggregation. Haematological parameters were examined in rats vaccinated with GluN1. Platelet effects of a mouse monoclonal antibody targeting the glycine-binding region of GluN1 (GluN1-S2) were tested in assays of platelet activation, aggregation and thrombus formation. The epitope of anti-GluN1-S2 was mapped and the mechanism of antibody action modelled using crystal structures of GluN1. Our work found that rats vaccinated with GluN1 had a mildly prolonged bleeding time and carried antibodies targeting mostly GluN1-S2. The monoclonal anti-GluN1-S2 antibody (from BD Biosciences) inhibited activation and aggregation of human platelets in the presence of adrenaline, adenosine diphosphate, collagen, thrombin and a protease-activated receptor 1-activating peptide. When human blood was flowed over collagen-coated surfaces, anti-GluN1-S2 impaired thrombus growth and stability. The epitope of anti-GluN1-S2 was mapped to α-helix H located within the glycine-binding clamshell of GluN1, where the antibody binding was computationally predicted to impair opening of the NMDAR channel. Our results indicate that anti-GluN1-S2 inhibits function of human platelets, including dense granule release and thrombus growth. Findings add to the evidence that platelet NMDARs regulate thrombus formation and suggest a novel mechanism by which anti-GluN1 autoantibodies limit stroke-induced neuronal damage.

## Keywords

Calcium, glutamate, ion channel, platelet inhibitor, stroke

## History

Received 23 October 2016
Revised 22 December 2016
Accepted 29 December 2016
Published online 22 February 2017

## Introduction

GluN1 (previously known as NR1 or NMDAR1) represents an obligate subunit of *N*-methyl-D-aspartate receptors (NMDARs) [1, 2]. Typical NMDARs combine two GluN1 subunits with another two GluN2 components (of which there are four possible; designated GluN2A to GluN2D). GluN3 subunits (GluN3A or GluN3B) may also be present, but are less common. The GluN1 subunits have important structural roles and bind glycine (NMDAR co-ligand); GluN2 subunits are regulatory and bind glutamate (main NMDAR ligand). In response to binding of glutamate and glycine, NMDARs facilitate intracellular influx of predominantly calcium ions ($Ca^{2+}$), kinetics of which are differentially regulated by the GluN2 subunits [2, 3].



Correspondence: Maggie L. Kalev-Zylinska, Department of Molecular Medicine and Pathology, University of Auckland, ACM 1142, Auckland, New Zealand. Tel: +6421337776. Fax: +6493677121. E-mail: m.kalev@auckland.ac.nz.

There is increasing evidence that similar to other peripheral tissues [4], platelets express NMDAR components but their roles remain unclear [5–11]. NMDARs have been shown to reduce [6, 7], increase [10] or have no influence [12] over different aspects of platelet function. Our previous work has demonstrated that blockers of open NMDAR channels (MK-801 and memantine) inhibit activation and aggregation of human platelets, although these effects required relatively high inhibitor concentrations [10].

Plasma glutamate levels are dynamically regulated by platelets that take it up from plasma using excitatory amino-acid transporters, store it in dense granules and then release it after aggregation [13–15]. In ischaemic stroke, glutamate levels rise, both in plasma and cerebrospinal fluid, due to its excessive release from the damaged brain and reduced re-uptake by activated platelets [16–18]. High glutamate levels overactivate neuronal NMDARs, leading to intracellular $Ca^{2+}$ overload and cell death [19, 20]. Our previous research focused on designing experimental therapies for ischaemic stroke that would interfere with overactive neuronal NMDARs. We developed a novel anti-GluN1 vaccine that when tested in rats generated high levels of anti-GluN1 antibodies and markedly reduced brain infarcts in a model of stroke [21]. We concluded that ischaemic breakdown of the blood–brain–barrier delivered anti-GluN1 antibodies to the region of stroke where antibodies interfered with overactive neuronal NMDARs, while normal brain was spared from unwanted side-effects. Such neuroprotective properties of anti-GluN1 antibodies may be relevant in humans, as up to 10% of healthy individuals and 20–40% of stroke patients carry non-pathogenic anti-GluN1 antibodies [22–27]. Some of such antibodies develop transiently after ischaemic stroke and react only with GluN1 breakdown products [22] but others, when present before the stroke, may reduce stroke damage [27].

The phenomenon of anti-GluN1-mediated stroke protection was confirmed in other models [28, 29], but we found the underlying mechanism difficult to elucidate. Early reports on NMDAR functionality in platelets [5–9] led us to hypothesise that the previously observed anti-GluN1-mediated stroke protection involved inhibition of platelet function. This hypothesis was examined in rats vaccinated with GluN1 followed by testing of antibody effects on human platelets, including under blood flow conditions equivalent to stenosed arteries. The results will demonstrate how epitope mapping of anti-GluN1 antibodies led us to a novel mechanism regulating human platelet function in the setting of thrombosis.

## Materials and methods

### Cloning and generation of recombinant peptides

Sequences encoding all extracellular regions of mouse GluN1 (amino acid [aa] numbers: 1–562 and 654–812) were fused with a 13-residue linker as previously reported (Figure 1A; [30]). The fusion was subcloned into *Bam*HI and *Not*I sites of a bacterial expression plasmid, pTriEx-1.1 (Novagen, Madison, WI). Sequences encoding full-length firefly luciferase were cloned as controls into *Nco*I and *Eco*RI sites of pTriEx-1.1. Both constructs contained histidine tags at the C-termini of protein-coding sequences.

Recombinant GluN1 (80 kDa) and luciferase (65 kDa) peptides were expressed in *Escherichia coli* BL21 (DE3) strain (Novagen) and purified by nickel affinity on a Profinia Protein Purification System (Bio-Rad, Hercules, CA) as before [22]. The GluN1 peptide was concentrated through a centrifugal filter device with a 50 kDa cut-off (Millipore, Darmstadt, Germany). Both peptides were dialysed against phosphate-buffered saline (PBS) in Slyde-A-Lyzer cassettes (ThermoFisher Scientific, Rockford, IL).

### Experiments in rats

Studies in rats were performed in accordance with the national legal requirements and institutional guidelines; all procedures were approved by the institutional Animal Ethics Committee (AEC/11/2006/R532). Male *Wistar* rats (initially 180–220 g) were housed in pairs in an animal facility under standard conditions (23 ± 1°C, 50 ± 5% humidity, 12 h light/dark cycle) and with free access to food and water. Recombinant GluN1, luciferase and vehicle only vaccines were injected subcutaneously into rats starting at 6 weeks of age. Vaccine priming was conducted using 100 μg of the recombinant peptides admixed 1:1 with an Alum adjuvant (ThermoFisher Scientific), followed by 6 fortnightly boosts with 50 μg peptides.

Bleeding time was measured in rats anaesthetised with 60 mg $kg^{-1}$ sodium pentobarbitone (PhoenixPharm, Auckland, New Zealand) injected intraperitoneally. At weeks 0 and 20, a distal 3 mm segment was cut from the tail, and the tail tip was blotted on a filter paper every 15 s. At week 10, a skin cut was made (0.5 cm long, 0.5 mm deep) along the tail vein, 5 cm from the previously cut tail tip, and blotted as above. The bleeding time was determined when filter paper was no longer stained with fresh blood.

Full blood counts were obtained from peripheral blood samples taken from a tail vein of rats anaesthetised with 5% isoflurane (Lunan Better Pharmaceutical, ShanDong, China). Tail was placed in warm water for 40 s, dried, swabbed with alcohol, and the tip punched with an 18-gauge needle. Free-flowing blood was collected into EDTA microtainer tubes (BD Biosciences, San Jose, CA). Blood counts were obtained within 6 h from collection on an XE-2100 automated haematology analyser (Sysmex, Kobe, Japan).

Plasma ferritin levels were measured using a Ferritin FTL Rat ELISA kit (Abcam, Cambridge, UK).

### Characterisation of anti-GluN1 antibody responses

Antibody levels were monitored by antigen-capture ELISA employing recombinant GluN1 and luciferase peptides injected as vaccines; blood was sampled fortnightly from tail veins of restrained, un-anaesthetised rats. The assay was performed essentially as before [22] except that o-phenylenediamine dihydrochloride (OPD) was used as a substrate.

To determine epitopes of anti-GluN1 antibody binding, antigen capture was modified to include a library of 74 synthetic peptides spanning all extracellular regions of GluN1 (Mimotopes, PepSets™, Melbourne, Australia; Supplemental Table S1). The 13 aa linker was included in the library, although it was not a part of the native protein. All synthetic peptides were 16 aa long containing hexamer repeats overlapping the adjacent peptides at both ends and a biotin label 5′.

Microtitre plates (Nunc MaxiSorp, ThermoFisher Scientific) were coated with streptavidin (5 μg per well), blocked with 5% skim milk (weight per volume [w/v]) and incubated with synthetic peptides (250 pmol per well). Pooled rat sera were applied in triplicate, diluted 1:200. Pools of human sera previously identified as anti-GluN1 positive or negative were used as controls (1:100). After an overnight incubation with primary antibodies, plates were washed and appropriate secondary antibodies applied for 3 h (all were peroxidase-conjugated and diluted 1:10 000; Sigma-Aldrich;Saint Louis, MO). Signals were developed using OPD. Full details of the method are in the Supplemental Material.

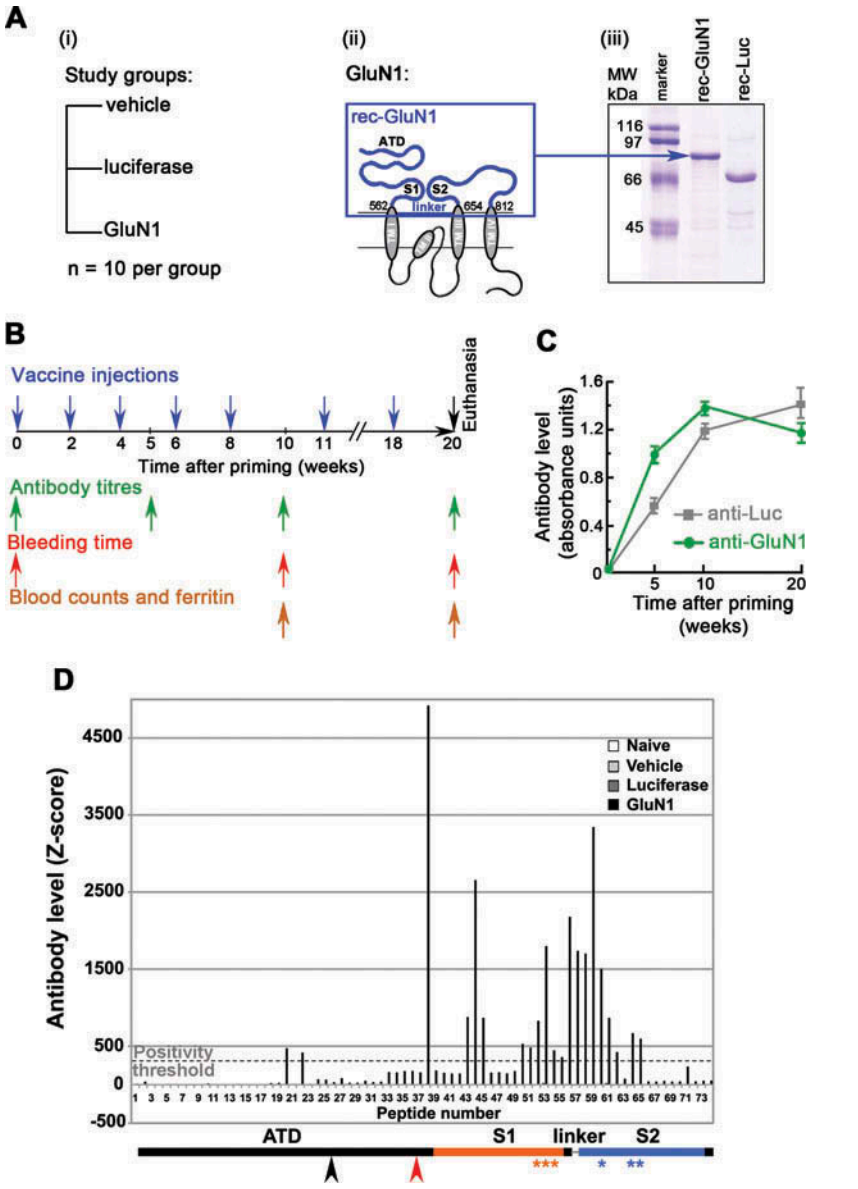


Figure 1. Vaccine design and antibody responses. (A) Study groups (A.i); recombinant GluN1 design (A.ii) and a Coomassie-blue-stained gel showing recombinant GluN1 and luciferase peptides (rec-GluN1 and rec-Luc) used in vaccination (A.iii). (B) Study time-line and study procedures. (C) Levels of anti-GluN1 and anti-Luc antibodies produced in vaccinated rats. Data points are mean ± SEM ($n$ = 10 per group). (D) Epitopes of anti-GluN1 antibody binding in vaccinated rats. Epitopes were mapped using 74 synthetic peptides spanning all extracellular regions of GluN1 (data are for pooled sera, $n$ = 10 per group; synthetic GluN1 peptides are numbered, sequences are in the Supplemental Table S1). Z-scores were calculated relative to negative control sera with the positivity threshold set greater than 2x SD from the mean of negative controls. No significant anti-GluN1 reactivities were detected in control rats (naïve, vehicle or luciferase vaccinated, hence bars for these groups are not visible). The following domains of the native GluN1 protein are marked: the amino-terminus (ATD), S1, S2, cleavage site for alteplase (black arrowhead; [29]), binding site for pathogenic anti-NMDAR antibodies that cause limbic encephalitis (red arrowhead; [52]) and residues that interact with glycine (orange and blue stars for S1 and S2, respectively; [35]). Abbreviations: Luc, luciferase; rec, recombinant.

## Experiments on human platelets

All work on human platelets was carried out in accordance with the Declaration of Helsinki on Ethical Principles for Medical Research Involving Human Subjects; all procedures were approved by two regional Human Ethics Committees (AKX/03/07/183 [Auckland] and CF07/0141 [Melbourne]). Written informed consent was obtained from all participants prior to testing. Platelet experiments were performed using samples from 34 healthy donors with a median age of 33 ± 9 years (standard deviation); 23 were women. Most donors were European, but included 7 Chinese, 3 Indian, 1 Samoan and 1 Māori. All donors were self-reported to be medication-free for at least 2 weeks prior to testing. Unless stated otherwise, blood was collected on 3.2% trisodium citrate (BD Biosciences).

Platelet rich and platelet poor plasma (PRP and PPP, respectively) were prepared and platelet aggregation examined by light transmission aggregometry (LTA) as before [10]. Four commercial anti-GluN1 antibody samples were screened for their abilities to inhibit platelet aggregation. Two were mouse monoclonals targeting 660–811 aa region of GluN1-S2 (MAB363, Millipore and BD556308, BD Biosciences); the other two targeted the GluN1 N-terminus: MAB1586 (Millipore; mouse monoclonal targeting 1–564 aa) and SC9058 (Santa Cruz, Dallas, TX; rabbit polyclonal targeting 19–318 aa). The exact epitopes were not known for any of the antibodies. Each antibody (1 μg $mL^{-1}$) was incubated with PRP (200 × $10^9$ $L^{-1}$ platelets) for 1 min prior to adding 10 μM adenosine diphosphate (ADP; Helena Laboratories, Beaumont, TX). Further experiments investigated effects of anti-GluN1-S2 (BD; 0.004–4 μg $mL^{-1}$) on platelet aggregation using an extended panel of agonists: adrenaline (5–10 μM), ADP (2.5–10 μM), collagen (0.5–1 μg $mL^{-1}$; all from Helena Laboratories), thrombin (0.25 U $mL^{-1}$; Sigma-Aldrich, Saint Louis, MO) and a protease-activated receptor 1-activating peptide (PAR1-AP; SFLLRN-$NH_2$; 7–15 μM; Abcam). Lowest effective concentrations of agonists were used for each platelet donor. Normal mouse immunoglobulin (IgG; Sigma-Aldrich) was used as a negative control.

To examine effects on platelet activation, anti-GluN1-S2 (1 μg $mL^{-1}$) was mixed with PRP in the presence of anti-CD62P-PE, PAC-1-FITC, anti-CD61-PerCP or appropriate isotype controls (all from BD Biosciences) and platelets were activated with ADP (1 or 2.5 μM). Data was acquired on LSRII (BD Biosciences) as in our previous studies [10, 31]. Platelets were gated based on forward and side scatter characteristics (FSC-A–SSC-A), verified by CD61 expression (based on CD61-PerCP–

FSC-A) and restricted to single cell events (based on both SSC-H–SSC-A and FSC-H–FSC-A; Supplemental Figure S1).

Surface binding of anti-GluN1-S2 was measured on platelets activated with thrombin (0.05–0.1 U $mL^{-1}$) and convulxin (100 ng $mL^{-1}$, Enzo Life Sciences, Farmingdale, NY) in the presence of integrilin to prevent platelet aggregation (50 μg $mL^{-1}$; Merck & Co, Kenilworth, NJ). The activation procedure and the analysis of GluN1 expression on CD62P-positive platelets were conducted based on the recently published method [32]. Briefly, PRP ($24 \times 10^9$ $L^{-1}$ final platelet concentration) was incubated with integrilin for 2 min and subsequently activated with either thrombin or convulxin for 15 min. Control platelets were processed the same way but contained no added activators nor inhibitors. Anti-GluN1-S2 or an isotype control (DAKOCytomation, Glostrup, Denmark) were applied and incubated with PRP for 30 min. Platelets were washed, incubated with secondary goat anti-mouse IgG-FITC, washed again and incubated with anti-CD62P-PE (both for 30 min). After a further wash, platelets were fixed with 0.2% (w/v) paraformaldehyde (PFA) and kept in the dark at 4°C until acquisition. The intracellular binding of anti-GluN1-S2 was examined in platelets permeabilised with IntraPrep™ (Beckman Coulter, Marseille, France).

Dense granule secretion was assessed from the levels of extracellular adenosine triphosphate (ATP) measured using an ATPlite Luminescence Detection System (Perkin-Elmer, Boston, MA) before and after platelet activation with ADP (0.5–10 μM), collagen (1 and 5 μg $mL^{-1}$; both from Helena Laboratories) and PAR1-AP (10–40 μM; Abcam). The procedure was conducted in 96-well white, clear bottom plates (Corning Inc, Corning, NY) according to manufacturer's instructions. PRP (with the platelet count adjusted to $200 \times 10^6$ $mL^{-1}$) was added to the reaction mixture at 1:5 dilution and platelets were activated in the presence of either anti-GluN1-S2 (BD Biosciences) or mouse control IgG (Sigma-Aldrich; both at 10 ng per 100 000 platelets). Luminescence was read on an EnSpire 2300 Multimode Plate Reader (Perkin-Elmer).

Immunocytochemistry was performed on platelets activated/aggregated with thrombin (0.1 U $mL^{-1}$, Sigma-Aldrich). Cytospins were prepared using Aerospray HaematologyPro (ELITech, Puteaux, France). Slides were fixed in 2% (w/v) PFA for 15 min and stained using the Novolink Polymer Detection System (Leica Biosystems, Newcastle, UK) as before [33]. The anti-GluN1-S2 antibody (MAB363, Millipore) and an isotype control were incubated overnight at 4°C. Staining was imaged using an Eclipse N*i* upright microscope (Nikon, Tokyo, Japan).

### Thrombus formation under flow conditions

Human whole blood was collected in hirudin (800 U $mL^{-1}$) and pre-incubated with either anti-GluN1-S2 (BD Biosciences) or mouse control IgG (Sigma-Aldrich; both at 10 μg $mL^{-1}$) for 15 min at 37°C. The blood was then mixed with the fluorescent membrane stain 3,3′-dihexyloxacarbocyanine iodide ($DiOC_6$, 1 μg $mL^{-1}$) and flowed over collagen (50 μg $mL^{-1}$) coated microslides at 1800 $s^{-1}$ for 3 min, followed by a 4 min wash-out with Tyrode's buffer, essentially as before [34]. Platelet deposition and thrombus volume were monitored in real-time by the acquisition of continuous Z-series throughout the assay and calculated offline using NIS software (Nikon).

### Characterisation of the anti-GluN1-S2 epitope

The epitope of anti-GluN1-S2 (BD) was identified as described above for rat sera (further details are in the Supplemental Methods). Anti-GluN1-S2 was diluted 1:500 and peroxidase-conjugated anti-mouse secondary antibody 1:10 000 (Sigma-Aldrich).

Western blotting on platelet proteins was conducted as described before [10]. Protein samples (30 μg per lane) were separated by 10% SDS-polyacrylamide gel electrophoresis and transferred to a nitrocellulose membrane (Hybond-ECL, Amersham, Piscataway, NJ). The anti-GluN1-S2 antibody was incubated with membranes overnight (1:1000–3000). To verify specificity of anti-GluN1-S2 binding, antibodies were pre-absorbed with recombinant GluN1 peptides added in excess according to the equation: $n$(antigen) = $n$(antibody) × 2[molecular weight(antigen) /molecular weight(antibody)]. The mixtures were incubated at 4°C overnight with constant rotation and spun at 10 000 rpm for 5 min prior to further use. Signals were developed using ECLPlus (ThermoFisher Scientific) and imaged by a FujiFilm LAS-3000 phosphoimager (Life Science, Stamford, CT).

The epitope of anti-GluN1-S2 was visualised in 3D using the following X-ray crystal structures of GluN1: Protein Data Bank (PDB) entry 1PB7, complexed with glycine (active GluN1 conformation) and PDB 1PBQ, complexed with 5,7-dichlorokynurenic acid (DCKA; inactive GluN1 conformation) [35]. The crystal structures were superimposed using PyMol Molecular Graphics version 1.7.4 based on the S1S2 domain 1 of the GluN1 glycine-binding clamshell, chains A 4–140 and 251–285 aa [35]. Protein alignments were generated using Geneious version 8.1.4.

### Statistical analysis

Statistical analysis was conducted using GraphPad Prism for Windows (San Diego, CA). Mean differences between groups were analysed by independent-samples Student's $t$-test (two-tailed), one-way or two-way analysis of variance (ANOVA) for multiple groups, as appropriate. $p$ values less than 0.05 were considered statistically significant. Data are shown as mean ± standard error of the mean (SEM), except for the age of platelet donors reported as median ± standard deviation (SD)

## Results

### Rats vaccinated with recombinant GluN1 have prolonged bleeding time

Male *Wistar* rats were vaccinated subcutaneously with recombinant GluN1 peptides containing all extracellular regions of GluN1. Recombinant luciferase and vehicle only vaccines were used as negative controls ($n$ = 10 rats per group; Figure 1A). Seven doses of each vaccine were administered to rats over 18 weeks (Figure 1B). All rats gained weight at the same rate with no obvious systemic ill effects and no signs of bleeding (data not shown). Both peptides induced high levels of antibodies with similar titres between anti-GluN1 and luciferase vaccinated rats (Figure 1C). Epitopes of anti-GluN1 antibodies were mapped using a library of 74 synthetic peptides spanning all extracellular regions of GluN1. Similar to our earlier GluN1 vaccine that was neuroprotective [21], rats vaccinated with recombinant GluN1 peptides produced antibodies targeting mostly GluN1-S2 that contains sites for glycine binding (Figure 1D).

Haematological tests were performed in vaccinated rats in weeks 10 and 20 (Figure 2). Unexpectedly, we found that rats vaccinated with GluN1 had a mildly prolonged bleeding time, compared with both luciferase- and vehicle- injected controls (2.2-fold increase in week 20; $p < 0.001$; Figure 2A). Platelet counts and platelet volumes remained unaffected, excluding thrombocytopaenia as a cause (Figure 2B). GluN1-vaccinated rats also developed microcytic hypochromic anaemia typical of iron deficiency that was confirmed by reduced reticulocyte haemoglobin-equivalent (Ret-He) and low plasma ferritin in week 20 ($p < 0.05$; Figure 2B; Supplemental Tables S2 and S3). The

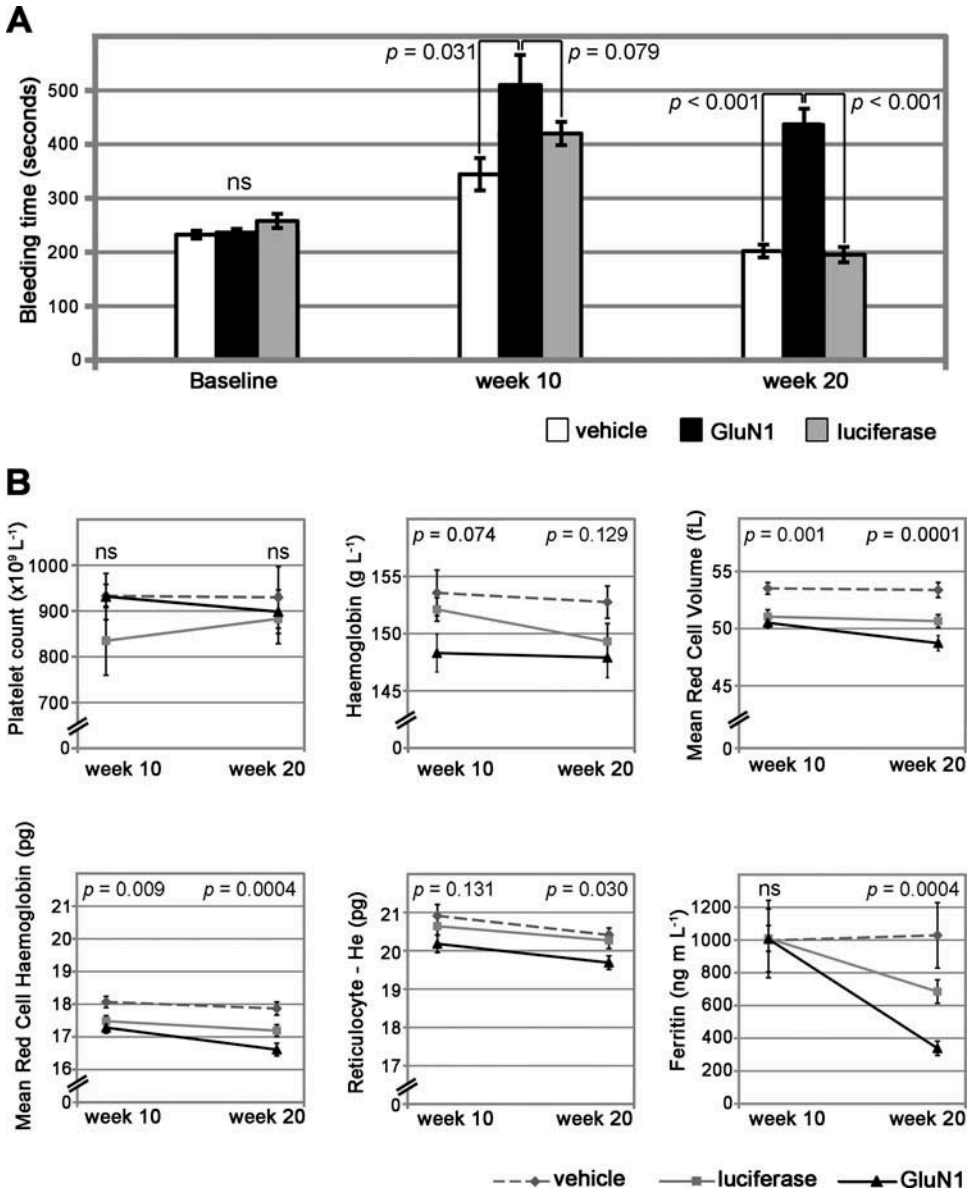


Figure 2. Haematological parameters in GluN1-vaccinated rats. Rats received fortnightly subcutaneous injections with recombinant GluN1 and luciferase peptides or a vehicle control. Bleeding time, peripheral blood counts and ferritin levels were tested after 10 and 20 weeks from vaccine priming. (A) Bleeding times are shown, measured from cut tails at baseline and week 20, and from a skin cut at week 10. (B) Line graphs highlight changes in selected haematological parameters occurring between weeks 10 and 20. Data points indicate mean ± SEM ($n$ = 10 per group). In A, Dunnett's *post-hoc* $p$ values are shown. In B, $p$ values indicate group differences; *post-hoc* values are in Supplemental Tables S2 and S3 (one-way ANOVA). Abbreviations: ns, non-significant; Reticulocyte-He, Reticulocyte Haemoglobin equivalent.

development of iron deficiency in GluN1-vaccinated rats confirmed that they lost more blood.

### Anti-GluN1-S2 antibody inhibits platelet function

Four commercial antibodies targeting various extracellular regions of human GluN1 (listed in Materials and Methods) were screened for their ability to inhibit human platelet aggregation in the presence of 10 μM ADP. Of these, the anti-GluN1-S2 mouse monoclonal antibody (BD556308, BD Biosciences) provided the strongest level of inhibition (screen data not shown) and its effects were tested further (Figures 3–6). In the flow cytometry-based assay of platelet activation (using 1 and 2.5 μM ADP), anti-GluN1-S2 (1 μg $mL^{-1}$) provided little interference. Nevertheless, compared with mouse control IgG, CD62P exposure mildly declined accompanied by a reciprocal increase in PAC-1 binding of 6.2 ± 3.6% ($p$ < 0.05; Figure 3A). The biological significance of these small changes is unclear, but the results suggested that anti-GluN1-S2 interfered with some aspects of platelet activation, such as granule release, but not with the conformational change of glycoprotein (GP) αIIbβ3.

In comparison to subtle effects on platelet activation, platelet aggregation was strongly inhibited by anti-GluN1-S2 both at 0.4 and 4 μg $mL^{-1}$ (Figure 3B; Supplemental Figure S2). In the presence of adrenaline (5–10 μM) and ADP (2.5–10 μM), aggregation was virtually abrogated (primary wave only remained). With collagen (0.5–1 μg $mL^{-1}$), effects of anti-GluN1-S2 were weaker but aggregation was still reduced to 42 ± 9% of controls ($p$ = 0.005). The degree of inhibition was most variable in the presence of thrombin (0.25 U $mL^{-1}$) and PAR1-AP (7–15 μM), ranging from 4 to 95% between donors (overall 29 ± 9% inhibition; $p$ = 0.026). In addition to

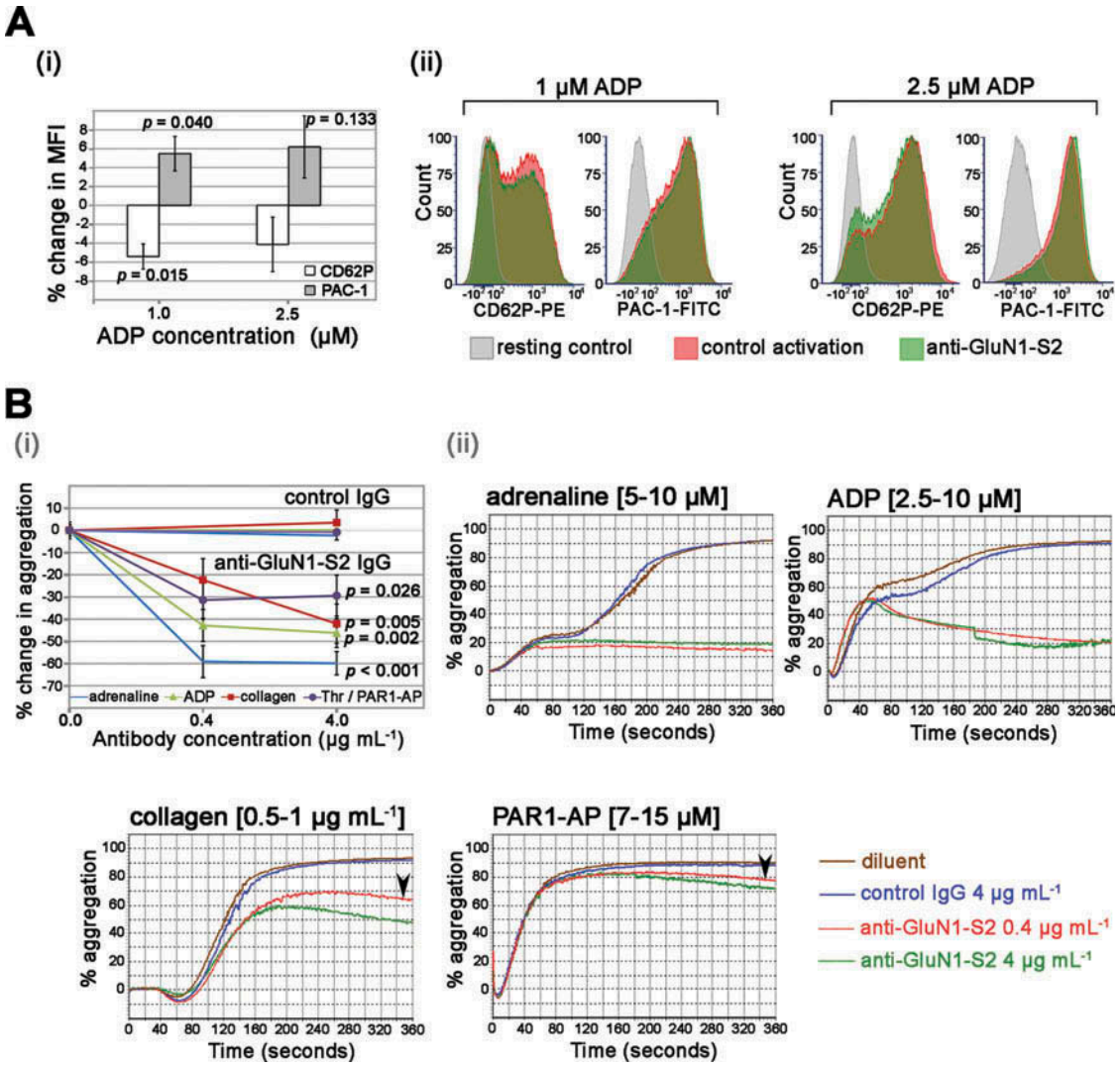


Figure 3. Effects of anti-GluN1-S2 on platelet activation and aggregation. (A) Human platelets were activated with ADP (1 and 2.5 μM) in the presence or absence of anti-GluN1-S2 (1 μg mL$^{-1}$). (A.i) Relative changes in the CD62P exposure and PAC-1 binding imposed by anti-GluN1-S2 (1 μg mL$^{-1}$) graphed as percentage change in MFI (mean fluorescence intensity) compared with mouse control IgG. Data points are mean ± SEM; $n = 5$ per group (7 donors; median age 29 ± 9 years; 3 women); $p$ values are shown (unpaired, two-tailed, Student's $t$-test). (A.ii) Histogram examples demonstrating CD62P and PAC-1 MFI occurring in the presence of anti-GluN1-S2 (green) compared with control activation (red) and resting platelets (grey). (B) Human platelets were pre-treated with either anti-GluN1-S2 (0.4 and 4 μg mL$^{-1}$) or control mouse IgG (4 μg mL$^{-1}$) and platelet aggregation was induced using adrenaline (5–10 μM), ADP (2.5–10 μM), collagen (0.5–1 μg mL$^{-1}$), thrombin (Thr; 0.25 U mL$^{-1}$) or PAR1-AP (7–15 μM). (B.i) Relative changes in aggregation area under the curve (AUC) imposed by anti-GluN1-S2 graphed as percentage change in AUC compared with mouse control IgG. Data points are mean ± SEM; $n = 5$–9 per group (19 donors; median age 29 ± 10 years; 11 women); $p$ values are shown (one-way ANOVA with Dunnett's *post-hoc*). (B.ii) Representative examples of aggregation traces for the agonists indicated; arrowheads point to signs of platelet disaggregation over time. MFI, mean fluorescence intensity.

a reduction in the maximum amplitude of aggregation, mild platelet disaggregation was also seen over time, in particular in the presence of collagen and PAR1-AP (Figure 3B.ii, arrowheads; Supplemental Figure S2). In the presence of adrenaline and ADP, the inhibitory effects of anti-GluN1-S2 persisted down to 0.01 μg mL$^{-1}$, indicating potent inhibition by the antibody (Supplemental Figure S3).

The strong inhibition of ADP-induced platelet aggregation by anti-GluN1-S2 raised the question whether this antibody inhibits dense granules release. This possibility was examined by measuring levels of ATP, that is abundantly stored in dense granules, before and after platelet activation with ADP (0.5–10 μM), PAR1-AP (10–40 μM) and collagen (1 and 5 μg mL$^{-1}$) in the presence of either anti-GluN1-S2 or control IgG. The results revealed that ATP levels declined by up to 47 ± 9% when platelets were activated with ADP ($p < 0.001$), consistent with the inhibition of dense granules release (Figure 4A). The effect was weaker in the presence of PAR1-AP (17 ± 5% reduction; $p < 0.05$) and not detected in the presence of collagen (Figure 4B and 4C), suggesting dependency on the agonist/strength of activation.

## Anti-GluN1-S2 inhibits thrombus formation under flow conditions

The effect of anti-GluN1-S2 on thrombus formation was examined in real-time using a whole blood thrombosis assay where platelet thrombi were formed on collagen-coated glass

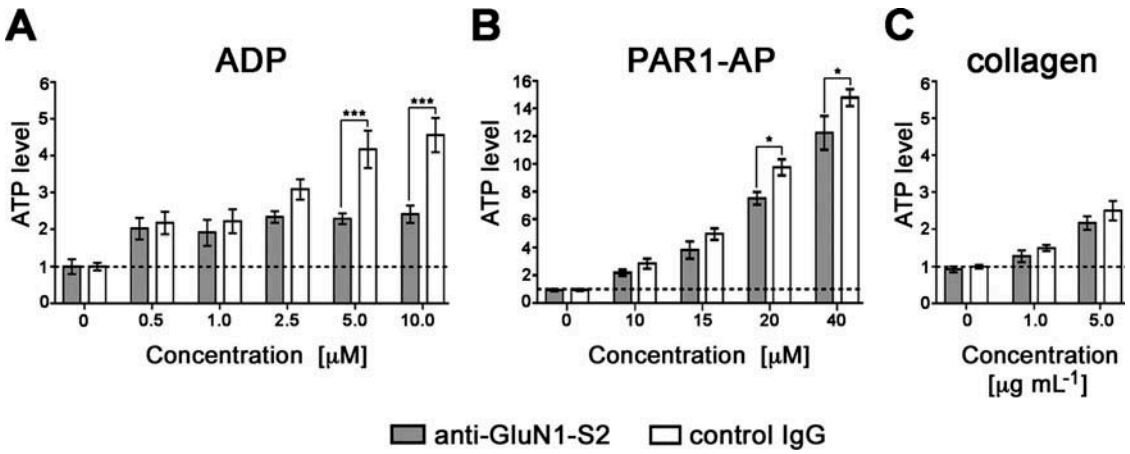


Figure 4. Effects of anti-GluN1-S2 on ATP release. Human platelets were activated with ADP (0.5–10 μM; A), PAR1-AP (10–40 μM; B) and collagen (1 and 5 μg $mL^{-1}$; C) in the presence of anti-GluN1-S2 or mouse control IgG (both at 10 ng per 100 000 platelets). Bars indicate relative ATP levels compared with non-activated controls. Data points are mean ± SEM; $n$ = 3–4 per group (6 donors; median age 30 ± 8 years; 3 women); Statistical significance is shown (*$p < 0.05$, ***$p < 0.001$; two-way ANOVA with Dunnett's *post-hoc*); other differences were not statistically significant.

microslides as described before [34]. This revealed that pre-treatment of human blood with anti-GluN1-S2 decreased the total volume of thrombus deposited on the slides, when compared with effects of a control mouse IgG ($p < 0.01$, $n = 6$; Figure 5A and 5B). Detailed analysis of thrombus formation kinetics demonstrated that the initial platelet deposition and early thrombus growth were largely unaffected by anti-GluN1-S2, but peak thrombus formation was impaired, which persisted throughout the thrombus consolidation period and subsequent buffer perfusion (Figure 5C). Video analysis suggested that the decrease in thrombus size was due to impaired adhesion of platelets recruited into late-stage thrombi in the presence of anti-GluN1-S2 (Supplemental Videos S1 and S2). The reduction in thrombus growth detected in flowing human blood was in keeping with the reduced maximum aggregation and platelet disaggregation demonstrated by LTA, as shown in Figure 3B and Supplemental Figure S2.

### Anti-GluN1-S2 binds on a small population of activated platelets

GluN1 was not reliably detected on the surface of resting platelets using membrane biotinylation (data not shown) and flow cytometry (Figure 6A and as previously reported [10]). Further testing was therefore conducted using platelets activated with thrombin (0.1 U $mL^{-1}$) and convulxin (100 ng $mL^{-1}$) in the presence of integrilin (50 μg $mL^{-1}$) to prevent platelet aggregation. These experiments found that anti-GluN1-S2 co-localised with CD62P on the surface of a small population of activated platelets (the overall mean 4.7 ± 1.7%; Figure 6B), despite the fact that the majority of platelets became positive for CD62P after activation with thrombin and convulxin. The anti-GluN1-S2 binding on the surface of platelets correlated with the strength of platelet activation but combining thrombin and convulxin did not obviously increase surface binding of anti-GluN1-S2 (data not shown).

Activated or aggregated platelets were also spun onto slides and GluN1 immunocytochemistry was performed (Figure 6C). Without prior activation, the intracellular GluN1 staining was punctate and widely distributed inside platelets, which changed after activation to a stronger concentric pattern but remained mostly intracellular. The strongest GluN1 staining was detected on the surface of platelet aggregates (Figure 6C). This dynamic immunocytochemistry pattern suggested activation-dependent GluN1 re-distribution in platelets, consistent with findings by flow cytometry (Figure 6B) and previous electron microscopy [10].

The specificity of anti-GluN1-S2 antibody binding to platelet GluN1 was confirmed on Western blots. The reactivity of the antibody with the 120 kDa platelet protein, consistent with platelet GluN1, was virtually abrogated after the antibody was pre-absorbed with recombinant GluN1 peptides (Figure 6D).

### Binding of anti-GluN1-S2 is predicted to inhibit NMDAR channel opening

The epitope of anti-GluN1-S2 (BD) was mapped to the following synthetic peptide: NYESAAEAIQAVRDNK (Supplemental Table S1; Supplemental Figure S4). This sequence is located at the end of exon 16 and beginning of exon 17 of human GluN1. The epitope is highly conserved between human, mouse and rat GluN1 proteins (Figure 7A) and shows no synergy with other GluN2 or GluN3 sequences (Figure 7B).

The epitope of anti-GluN1-S2 was visualised within two crystal structures of GluN1, complexed with either glycine (PDB entry 1PB7, carrying active GluN1 conformation) or DCKA (PDB entry 1PBQ, carrying inactive GluN1 conformation; Figure 7C). The epitope sequence was located on α-helix H of the glycine-binding region shaped as a clamshell. In the presence of glycine, α-helix H relocated upwards, which is known to close the GluN1 clamshell and open (activate) the NMDAR channel (Figure 8A) [35, 36]. Further examination in PyMol predicted that binding of anti-GluN1-S2 could impede the upward movement of α-helix H, thus preventing the GluN1 clamshell closure and stabilising the NMDAR channel in an inactive (closed) conformation (Figure 8B).

## Discussion

This study demonstrates that anti-GluN1-S2 antibodies inhibit function of human platelets *in vitro* and associate with prolonged bleeding time in GluN1-vaccinated rats. The monoclonal anti-GluN1-S2 antibody (from BD Biosciences) interfered with platelet aggregation in the presence of all agonists tested and caused platelet disaggregation. In keeping with this, the initial thrombus formation over collagen-coated surfaces was unaffected but peak thrombus growth was reduced and over time, platelets were seen to peel off the initial thrombi. The epitope of anti-GluN1-S2 was located within α-helix H of the GluN1 glycine-binding clamshell.

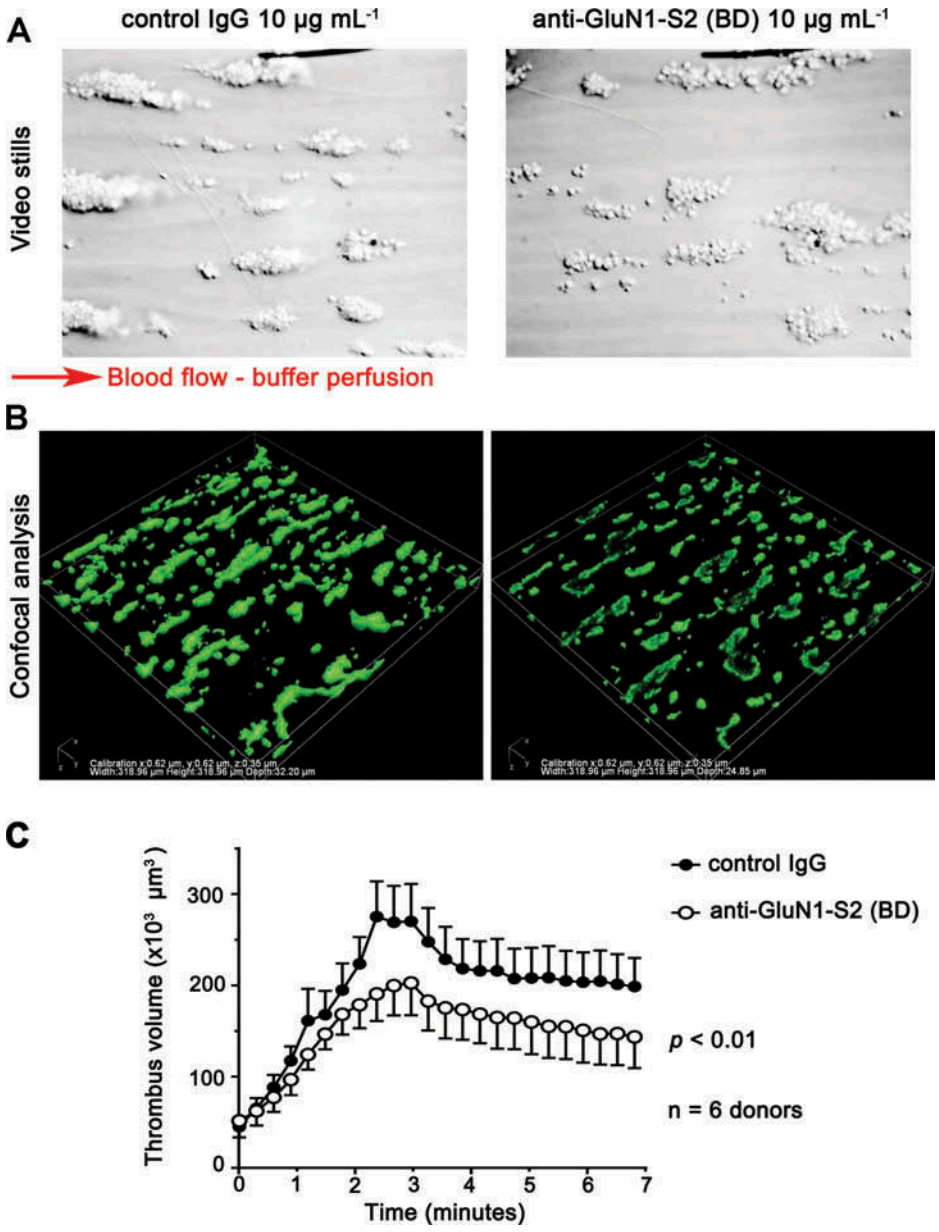


Figure 5. Anti-GluN1-S2 inhibits thrombus formation under flow conditions. Human whole blood was pre-treated with either anti-GluN1-S2 or control mouse IgG (both at 10 µg $mL^{-1}$) and perfused over microcapillary slides coated with type I collagen at a shear rate of 1800 $s^{-1}$. (A) Representative video stills taken at 7 min showing thrombi of reduced density in the presence of anti-GluN1-S2. (B) Representative Z-series stacks of $DiOC_6$-labelled thrombi formed after 7 min and imaged via confocal microscopy showing the smaller overall size and lower density of thrombi formed in the presence of anti-GluN1-S2. (C) Total average thrombus volume ($\mu m^3$) in one continuous field of view over the full experiment, determined from confocal-based reconstructions. Data are mean ± SEM of $n = 6$ independent experiments (6 donors; median age 29 ± 9 years; 4 women). $p < 0.01$ (unpaired, two-tailed, Student's *t*-test).

Structural modelling predicted that binding of anti-GluN1-S2 impaired NMDAR channel opening by stabilising the glycine-binding clamshell in an open conformation.

To our knowledge, this is the first study to report that anti-GluN1-S2 antibodies inhibit platelet function, including dense granule release and thrombus growth, which strengthens evidence for the NMDAR functionality in platelets and may help explain previous stroke-limiting effects of anti-GluN1 antibodies in rodents and humans [21, 27–29].

There is increasing evidence that human platelets contain functional NMDARs [5–11]. Platelets bind radiolabelled glutamate (NMDAR agonist) and MK-801 (NMDAR antagonist) [5, 6]. The presence of GluN1 in platelets was first shown by Hitchcock et al. using immunocytochemistry [9] and then by us using flow cytometry and Western blotting [10]. Our previous quantitative RT-PCR revealed that platelets contain transcripts for GluN1, GluN2A and GluN2D (products of their respective *GRIN1, GRIN2A* and *GRIN2D* genes). Recent independent transcriptomic analysis of the ion channelome in human platelets confirmed that platelets carry transcripts of *GRIN2D* and *GRINA* [11]. Emerging data suggest that platelet NMDARs are distinct from their neuronal counterparts, including different subunit composition [8–11], agonist-preferring state [5, 6] and sequestration inside resting platelets [10], features that likely impact our ability to detect NMDAR effects in different platelet function assays.

Glutamate is getting increasingly recognised as a late platelet agonist [37]. Previous studies demonstrated that glutamate amplifies platelet activation through two other types of ionotropic glutamate receptors, both of which were $Ca^{2+}$ impermeable: α-

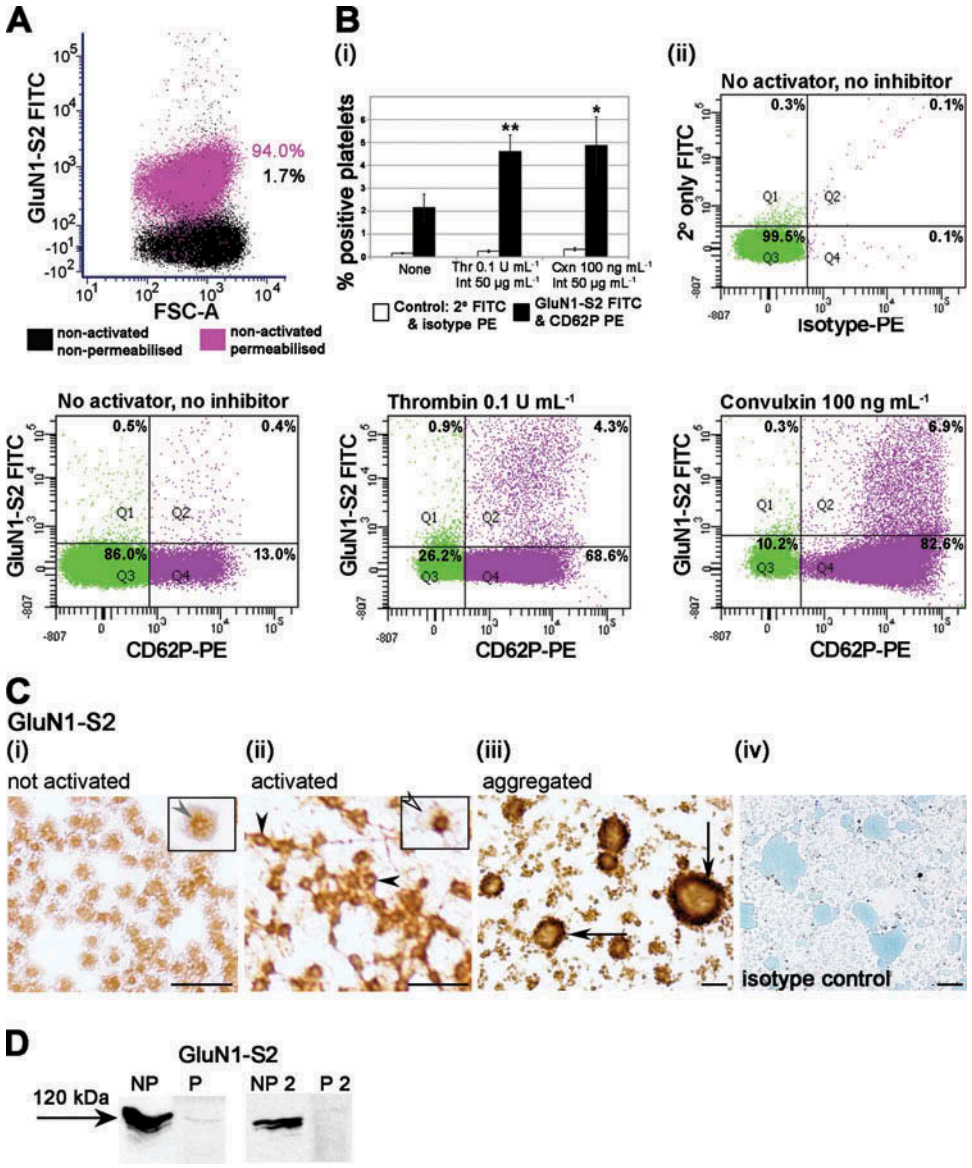


Figure 6. Platelet binding of anti-GluN1-S2. (A) Platelets were washed and anti-GluN1-S2 binding examined before (black) and after (pink) permeabilisation with IntraPrep™. A representative scatter-plot is shown indicating percentages of platelets that bound anti-GluN1-S2 under these conditions. (B) Unwashed platelets were activated with thrombin (0.1 U $mL^{-1}$) or convulxin (100 ng $mL^{-1}$) and tested for surface binding of anti-GluN1-S2. (B.i) Bars showing percentages of activated platelets expressing surface GluN1 under conditions of activation as indicated ($n$ = 3–5 per group; 5 donors; median age 31 ± 9 years; 3 women). Thr, thrombin; Cxn, convulxin; Int, integrilin. Statistical significance is shown (*$p < 0.05$, **$p < 0.01$; one-way ANOVA with Dunnett's *post-hoc*). (B.ii) Representative examples of flow cytometry scatter-plots demonstrating preferential binding of anti-GluN1-S2 on the subpopulations of activated platelets. (C) Representative GluN1 immunocytochemistry images showing: (C.i) diffuse and punctate intracellular GluN1 staining in platelets not previously exposed to an agonist (grey arrowhead); (C.ii) enhanced but still predominantly intracellular GluN1 staining in activated platelets (black arrowheads; a white arrowhead points to the surface of a platelet); (C.iii) strong GluN1 staining on the surface of small platelet aggregates (arrows). Scale bars: 10 µM. (D) Western blots showing binding of anti-GluN1-S2 to the 120 kDa platelet protein consistent with full-length GluN1 (arrow); marked reduction in binding is seen after the antibody was pre-absorbed with recombinant GluN1 peptides. NP, not pre-absorbed; P, pre-absorbed; 2 refers to a biological repeat.

amino-3-hydroxy-5-methyl-4-isoxazolepropionic (AMPA) and kainate [12, 38]. In comparison, NMDA has been shown to increase $Ca^{2+}$ concentrations inside platelets but inhibit platelet aggregation in the presence of low concentrations of agonists [6, 7]. Competitive NMDAR antagonists, CPP and D-AP5 (3-[2-carboxypiperazin-4-yl]propyl-1-phosphonic acid and D(−)-2-amino-5-phosphonopentanoic acid, respectively) did not affect platelet function [10, 12], likely because they needed to compete with saturating concentrations of glutamate and other agonists. In steady state plasma, glutamate concentrations range from 30 to 100 µM but rise >300 µM after platelet aggregation [12, 15, 39]. In our previous experiments, un-competitive NMDAR blockers (MK-801 and memantine) inhibited platelet aggregation from 100 µM [10], and antibody effects described in this study are consistent.

Our results do not diminish the importance of previous discoveries by other investigators that AMPA and kainate receptors regulate glutamate effects in platelets [12, 38]. In fact, our data adds to the body of evidence that the glutamatergic system is functional in platelets and involves all three types of ionotropic glutamate receptors previously characterised in the brain (AMPA, kainate and NMDA receptors). AMPA receptors (AMPARs) facilitate influx of $Na^{+}$ across the plasma membrane both in neurons and platelets, which causes depolarisation required for the NMDAR activation [2, 12]. Because AMPARs act upstream of the NMDARs, and AMPAR inhibitors abrogate platelet

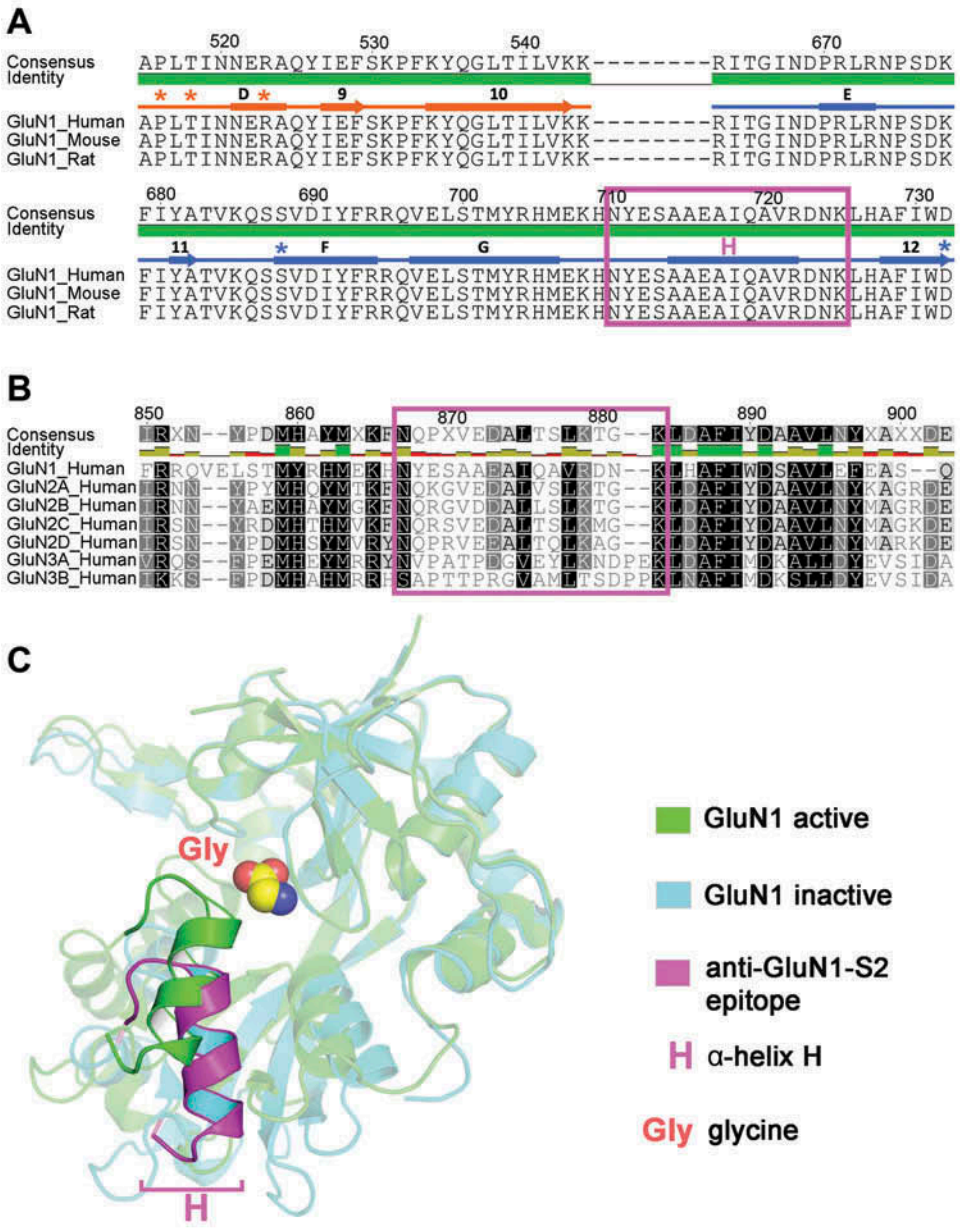


Figure 7. Characterisation of the anti-GluN1-S2 epitope. Sequence alignments of human GluN1-S2 against mouse and rat GluN1 (A) and against other human GluN2 and GluN3 proteins (B). The following NCBI accession numbers were used: NM_007327.3 (human GluN1), X63255.1 (rat GluN1), NM_008169.3 (mouse GluN1), NM_000833.4 (human GluN2A), NM_000834.3 (human GluN2B), NM_000835.4 (human GluN2C), NM_000836.2 (human GluN2D), NM_133445.2 (human GluN3A) and NM_138690.1 (human GluN3B). Arrows mark β-strands, rectangles α-helices, stars indicate glycine-interracting residues (orange for GluN1-S1 and blue for GluN1-S2; designated as in [35]). The epitope of anti-GluN1-S2 co-localises with α-helix H (framed in pink). (C) Two GluN1-S1S2 crystal structures are superimposed: 1PB7 (active GluN1 conformation; apple green) and 1PBQ (inactive GluN1 conformation; light blue). The anti-GluN1-S2 epitope is shown in pink on the inactive GluN1 structure. The front view of α-helix H emphasises the conformational rearrangement that occurs upon glycine (Gly) binding (α-helix H relocates upwards – cf upper green with lower pink-on-blue).

aggregation [12], we could not reliably determine additional effects of anti-GluN1-S2 in the presence of AMPAR inhibitors. We will pursue potential independent roles of AMPARs and NMDARs in transgenic mice with platelet-specific NMDAR deletion that we recently generated (data not shown). This transgenic mouse model will also allow us to determine if NMDAR modulation affects surface expression of major platelet glycoproteins, as short-term *in vitro* experiments with the antibody incubations cannot rule out such changes.

Our study also has other limitations. We have not examined thrombosis and haemostasis in GluN1-vaccinated rats nor tested effects of anti-GluN1-S2 in a stroke model. The stroke protective effects of anti-GluN1 antibodies were concluded from previous studies, including our own [21, 28, 29]. The mechanism through which anti-GluN1 antibodies regulate platelet function was modelled, but remains to be empirically tested.

We observed that binding of anti-GluN1-S2 on the surface of platelets required strong activation. The exact trigger for GluN1 externalisation is however unknown, as anti-GluN1-S2 bound only on a very small proportion of CD62P-positive platelets. Recent work revealed that upon strong activation, subpopulations of platelets become necrotic providing procoagulant surface for thrombus formation [32]. Considering that NMDAR overactivation links with necrosis in neurons [19, 20], studies into a similar link in activated platelets may be informative.

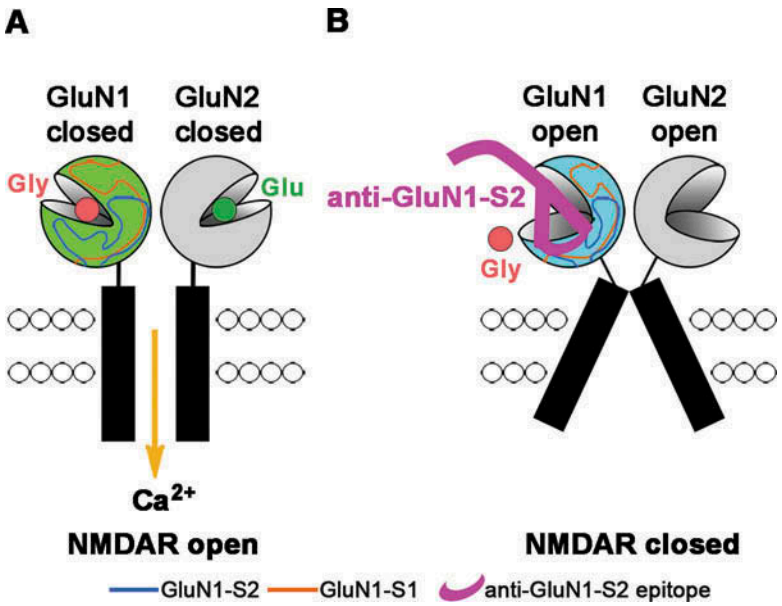


Figure 8. Proposed mechanism of the NMDAR inhibition by anti-GluN1-S2. (A) Agonist-binding domains of GluN1 and GluN2 are drawn as clamshells. When glycine binds, GluN1 clamshell closes (green), which contributes towards the opening of the NMDAR channel [36]. (B) Binding of anti-GluN1-S2 to α-helix H is predicted to inhibit clamshell closure (blue) and thus prevent NMDAR channel opening and receptor activation. Abbreviations: Gly, glycine; Glu, glutamate.

The functional effects of anti-GluN1-S2 antibodies we found include interference with dense granules release and induction of platelet disaggregation. Under arterial shear rates (1800 $s^{-1}$), anti-GluN1-S2 restricted thrombus growth resulting in smaller and less stable thrombi. These effects are important in ischaemic stroke. By limiting thrombus growth and facilitating thrombus breakdown, anti-GluN1 antibodies may help re-open cerebral arteries. Normal activation of GP αIIbβ3 in the presence of anti-GluN1-S2 suggested that NMDAR modulation spares resting platelets; however somewhat contrary to this, rats vaccinated with GluN1 had more bleeding. Repeat venipunctures may have contributed to greater loss of blood in vaccinated rats but a direct antibody effect on resting platelets cannot be excluded.

Others [7] and we [10] have already shown that glutamate and NMDA increase intra-platelet $Ca^{2+}$ levels, implying that platelet NMDARs operate as $Ca^{2+}$ channels. Previous observations were made in resting platelets, so likely underestimated NMDAR functionality; further testing of $Ca^{2+}$ fluxes in activated platelets should be more informative. The initial platelet activation culminates in the release of $Ca^{2+}$ stored in the dense tubular system (DTS) [40]. The emptying of stores initiates store-operated $Ca^{2+}$ entry (SOCE), primarily through the interaction of STIM1 with Orai1 channels [41]. However, SOCE takes up to 15 s to be completed [42], and its lack does not prevent prolonged $Ca^{2+}$ influx, platelet activation [43–46] or thrombin generation [47], indicating that other mechanisms of $Ca^{2+}$ entry also exist and can compensate. Of those, P2X1, canonical transient receptor potential 6 (TRPC6) and nicotinic cholinergic channels are known [48–50], but further mechanisms remain to be elucidated.

We propose that the following sequence of events applies under high shear rates. Stable adhesion of platelets to subendothelial collagen requires early interactions through GP VI and α2bβ1, and to von Willebrand factor through GP Ibα and αIIbβ3 [51]. The resultant downstream signalling mobilises $Ca^{2+}$ from the DTS, promoting granule secretion followed by high-affinity interactions between GP αIIbβ3 and fibrinogen. Thrombus growth and stability depend on prolonged $Ca^{2+}$ influx assisted by SOCE [44, 45, 51]. We speculate that NMDARs contribute to SOCE supporting platelet activation and thrombus growth but do not primarily interfere with earlier events of platelet adhesion and aggregation. Such late NMDAR effects are of clinical interest, as NMDAR inhibition may help restrict arterial thrombosis without disturbing early haemostasis. Further studies to determine mechanisms through which NMDARs contribute to $Ca^{2+}$ homeostasis and thrombus growth are warranted.

In conclusion, anti-GluN1-S2 antibodies interfere with platelet aggregation and thrombus formation under flow conditions, which may help explain previously reported stroke-limiting effects of anti-GluN1 antibodies in rodents and humans. Our findings strengthen evidence that platelet NMDARs are functional, justifying further work to examine NMDAR involvement in platelet $Ca^{2+}$ signalling and arterial thrombosis.

## Acknowledgments

We are grateful to Dr George Chan for supporting our use of a platelet aggregometer at LabPlus; Vivienne Muffty and Soakimi Pouhila assisted with platelet aggregation studies. Drs Kevin Little and Jerry Wong cloned recombinant GluN1 and luciferase constructs, respectively. Daying Wen helped produce recombinant GluN1 peptides. Special thanks goes to anonymous donors who provided blood for this work.

## Declaration of interest

The authors report no conflicts of interest.

The work was funded by Royal Society of New Zealand (Marsden Fast Start; UOA0903), Foundation for Research Science and Technology (UOAX0212) and Freemasons New Zealand (PJ Smith Travelling Fellowship to MLK-Z).

## Supplemental material

Supplemental data for this article can be accessed on the publisher's website.

## Notes on contributor

Taryn N. Green, Justin R. Hamilton, Marie-Christine Morel-Kopp, Zhaohua Zheng, Ting-Yu T. Chen, James I. Hearn, Peng P. Sun, Jack U. Flanagan, Deborah Young, P. Alan Barber, Matthew J. During, Christopher M. Ward, and Maggie L. Kalev-Zylinska. Published with license by Taylor & Francis.

## ORCID

Justin R. Hamilton http://orcid.org/0000-0001-7554-6727

Marie-Christine Morel-Kopp http://orcid.org/0000-0003-4795-1746
James I. Hearn http://orcid.org/0000-0002-3988-2659
Deborah Young http://orcid.org/0000-0003-1085-2824
P. Alan Barber http://orcid.org/0000-0003-2469-9023
Maggie L. Kalev-Zylinska http://orcid.org/0000-0001-8378-8048

## References

1. Collingridge GL, Olsen RW, Peters J, Spedding M. A nomenclature for ligand-gated ion channels. Neuropharmacology 2009;56:2–5.
2. Traynelis SF, Wollmuth LP, McBain CJ, Menniti FS, Vance KM, Ogden KK, Hansen KB, Yuan H, Myers SJ, Dingledine R. Glutamate receptor ion channels: structure, regulation, and function. Pharmacol Rev 2010;62:405–496.
3. Paoletti P, Bellone C, Zhou Q. NMDA receptor subunit diversity: impact on receptor properties, synaptic plasticity and disease. Nat Rev Neurosci 2013;14:383–400.
4. Hogan-Cann AD, Anderson CM. Physiological roles of non-neuronal NMDA receptors. Trends Pharmacol Sci 2016;37:750–767.
5. Almazov VA, Popov Iu G, Gorodinskii AI, Mikhailova IA, Dambinova SA. [The sites of high affinity binding of L-[3H]glutamic acid in human platelets. A new type of platelet receptor?]. Biokhimiia 1988;53:848–852.
6. Franconi F, Miceli M, De Montis MG, Crisafi EL, Bennardini F, Tagliamonte A. NMDA receptors play an anti-aggregating role in human platelets. Thromb Haemost 1996;76:84–87.
7. Franconi F, Miceli M, Alberti L, Seghieri G, De Montis MG, Tagliamonte A. Further insights into the anti-aggregating activity of NMDA in human platelets. Br J Pharmacol 1998;124:35–40.
8. Genever PG, Wilkinson DJ, Patton AJ, Peet NM, Hong Y, Mathur A, Erusalimsky JD, Skerry TM. Expression of a functional N-methyl-D-aspartate-type glutamate receptor by bone marrow megakaryocytes. Blood 1999;93:2876–2883.
9. Hitchcock IS, Skerry TM, Howard MR, Genever PG. NMDA receptor-mediated regulation of human megakaryocytopoiesis. Blood 2003;102:1254–1259.
10. Kalev-Zylinska ML, Green TN, Morel-Kopp MC, Sun PP, Park YE, Lasham A, During MJ, Ward CM. N-methyl-D-aspartate receptors amplify activation and aggregation of human platelets. Thromb Res 2014;133:837–847.
11. Wright JR, Amisten S, Goodall AH, Mahaut-Smith MP. Transcriptomic analysis of the ion channelome of human platelets and megakaryocytic cell lines. Thromb Haemost 2016;116:272–284.
12. Morrell CN, Sun H, Ikeda M, Beique JC, Swaim AM, Mason E, Martin TV, Thompson LE, Gozen O, Ampagoomian D, Sprengel R, Rothstein J, Faraday N, Huganir R, Lowenstein CJ. Glutamate mediates platelet activation through the AMPA receptor. J Exp Med 2008;205:575–584.
13. Begni B, Tremolizzo L, D'Orlando C, Bono MS, Garofolo R, Longoni M, Ferrarese C. Substrate-induced modulation of glutamate uptake in human platelets. Br J Pharmacol 2005;145:792–799.
14. Hoogland G, Bos IW, Kupper F, van Willigen G, Spierenburg HA, van Nieuwenhuizen O, de Graan PN. Thrombin-stimulated glutamate uptake in human platelets is predominantly mediated by the glial glutamate transporter EAAT2. Neurochem Int 2005;47:499–506.
15. Tremolizzo L, DiFrancesco JC, Rodriguez-Menendez V, Sirtori E, Longoni M, Cassetti A, Bossi M, El Mestikawy S, Cavaletti G, Ferrarese C. Human platelets express the synaptic markers VGLUT1 and 2 and release glutamate following aggregation. Neurosci Lett 2006;404:262–265.
16. Castillo J, Davalos A, Naveiro J, Noya M. Neuroexcitatory amino acids and their relation to infarct size and neurological deficit in ischemic stroke. Stroke 1996;27:1060–1065.
17. Castillo J, Davalos A, Noya M. Progression of ischaemic stroke and excitotoxic aminoacids. Lancet 1997;349:79–83.
18. Aliprandi A, Longoni M, Stanzani L, Tremolizzo L, Vaccaro M, Begni B, Galimberti G, Garofolo R, Ferrarese C. Increased plasma glutamate in stroke patients might be linked to altered platelet release and uptake. J Cereb Blood Flow Metab 2005;25:513–519.
19. Szydlowska K, Tymianski M. Calcium, ischemia and excitotoxicity. Cell Calcium 2010;47:122–129.
20. Forder JP, Tymianski M. Postsynaptic mechanisms of excitotoxicity: Involvement of postsynaptic density proteins, radicals, and oxidant molecules. Neuroscience 2009;158:293–300.
21. During MJ, Symes CW, Lawlor PA, Lin J, Dunning J, Fitzsimons HL, Poulsen D, Leone P, Xu R, Dicker BL, Lipski J, Young D. An oral vaccine against NMDAR1 with efficacy in experimental stroke and epilepsy. Science 2000;287:1453–1460.
22. Kalev-Zylinska ML, Symes W, Little KC, Sun P, Wen D, Qiao L, Young D, During MJ, Barber PA. Stroke patients develop antibodies that react with components of N-methyl-D-aspartate receptor subunit 1 in proportion to lesion size. Stroke 2013;44:2212–2219.
23. Hammer C, Stepniak B, Schneider A, Papiol S, Tantra M, Begemann M, Siren AL, Pardo LA, Sperling S, Mohd Jofrry S, Gurvich A, Jensen N, Ostmeier K, Luhder F, Probst C, Martens H, Gillis M, Saher G, Assogna F, Spalletta G, Stocker W, Schulz TF, Nave KA, Ehrenreich H. Neuropsychiatric disease relevance of circulating anti-NMDA receptor autoantibodies depends on blood-brain barrier integrity. Mol Psychiatry 2014;19:1143–1149.
24. Dahm L, Ott C, Steiner J, Stepniak B, Teegen B, Saschenbrecker S, Hammer C, Borowski K, Begemann M, Lemke S, Rentzsch K, Probst C, Martens H, Wienands J, Spalletta G, Weissenborn K, Stocker W, Ehrenreich H. Seroprevalence of autoantibodies against brain antigens in health and disease. Ann Neurol 2014;76:82–94.
25. Steiner J, Teegen B, Schiltz K, Bernstein HG, Stoecker W, Bogerts B. Prevalence of N-methyl-D-aspartate receptor autoantibodies in the peripheral blood: healthy control samples revisited. JAMA Psychiatry 2014;71:838–839.
26. Busse S, Busse M, Brix B, Probst C, Genz A, Bogerts B, Stoecker W, Steiner J. Seroprevalence of N-methyl-D-aspartate glutamate receptor (NMDA-R) autoantibodies in aging subjects without neuropsychiatric disorders and in dementia patients. Eur Arch Psychiatry Clin Neurosci 2014;264:545–550.
27. Zerche M, Weissenborn K, Ott C, Dere E, Asif AR, Worthmann H, Hassouna I, Rentzsch K, Tryc AB, Dahm L, Steiner J, Binder L, Wiltfang J, Siren AL, Stocker W, Ehrenreich H. Preexisting serum sutoantibodies against the NMDAR subunit NR1 modulate evolution of lesion size in scute ischemic stroke. Stroke 2015;46:1180–1186.
28. Macrez R, Obiang P, Gauberti M, Roussel B, Baron A, Parcq J, Casse F, Hommet Y, Orset C, Agin V, Bezin L, Berrocoso TG, Petersen KU, Montaner J, Maubert E, Vivien D, Ali C. Antibodies preventing the interaction of tissue-type plasminogen activator with N-methyl-D-aspartate receptors reduce stroke damages and extend the therapeutic window of thrombolysis. Stroke 2011;42:2315–2322.
29. Benchenane K, Castel H, Boulouard M, Bluthe R, Fernandez-Monreal M, Roussel BD, Lopez-Atalaya JP, Butt-Gueulle S, Agin V, Maubert E, Dantzer R, Touzani O, Dauphin F, Vivien D, Ali C. Anti-NR1 N-terminal-domain vaccination unmasks the crucial action of tPA on NMDA-receptor-mediated toxicity and spatial memory. J Cell Sci 2007;120:578–585.
30. Miyazaki J, Nakanishi S, Jingami H. Expression and characterization of a glycine-binding fragment of the N-methyl-D-aspartate receptor subunit NR1. Biochem J 1999;340(Pt 3):687–692.
31. Morel-Kopp MC, McLean L, Chen Q, Tofler GH, Tennant C, Maddison V, Ward CM. The association of depression with platelet activation: evidence for a treatment effect. J Thromb Haemost 2009;7:573–581.
32. Hua VM, Abeynaike L, Glaros E, Campbell H, Pasalic L, Hogg PJ, Chen VM. Necrotic platelets provide a procoagulant surface during thrombosis. Blood 2015;126:2852–2862.
33. Kamal T, Green TN, Morel-Kopp MC, Ward CM, McGregor AL, McGlashan SR, Bohlander SK, Browett PJ, Teague L, During MJ, Skerry TM, Josefsson EC, Kalev-Zylinska ML. Inhibition of glutamate regulated calcium entry into leukemic megakaryoblasts reduces cell proliferation and supports differentiation. Cell Signal 2015;27:1860–1872.
34. Mountford JK, Petitjean C, Putra HW, McCafferty JA, Setiabakti NM, Lee H, Tonnesen LL, McFadyen JD, Schoenwaelder SM, Eckly A, Gachet C, Ellis S, Voss AK, Dickins RA, Hamilton JR, Jackson SP. The class II PI 3-kinase, PI3KC2alpha, links platelet internal membrane structure to shear-dependent adhesive function. Nat Commun 2015;6:6535.

35. Furukawa H, Gouaux E. Mechanisms of activation, inhibition and specificity: crystal structures of the NMDA receptor NR1 ligand-binding core. EMBO J 2003;22:2873–2885.
36. Furukawa H, Singh SK, Mancusso R, Gouaux E. Subunit arrangement and function in NMDA receptors. Nature 2005;438:185–192.
37. Mahaut-Smith MP. The unique contribution of ion channels to platelet and megakaryocyte function. J Thromb Haemost 2012;10:1722–1732.
38. Sun H, Swaim A, Herrera JE, Becker D, Becker L, Srivastava K, Thompson LE, Shero MR, Perez-Tamayo A, Suktitipat B, Mathias R, Contractor A, Faraday N, Morrell CN. Platelet kainate receptor signaling promotes thrombosis by stimulating cyclooxygenase activation. Circ Res 2009;105:595–603.
39. Zhou Y, Qiu L, Xiao Q, Wang Y, Meng X, Xu R, Wang S, Na R. Obesity and diabetes related plasma amino acid alterations. Clin Biochem 2013;46:1447–1452.
40. Varga-Szabo D, Braun A, Nieswandt B. Calcium signaling in platelets. J Thromb Haemost 2009;7:1057–1066.
41. Varga-Szabo D, Braun A, Nieswandt B. STIM and Orai in platelet function. Cell Calcium 2011;50:270–278.
42. Muik M, Frischauf I, Derler I, Fahrner M, Bergsmann J, Eder P, Schindl R, Hesch C, Polzinger B, Fritsch R, Kahr H, Madl J, Gruber H, Groschner K, Romanin C. Dynamic coupling of the putative coiled-coil domain of ORAI1 with STIM1 mediates ORAI1 channel activation. J Biol Chem 2008;283:8014–8022.
43. Varga-Szabo D, Braun A, Kleinschnitz C, Bender M, Pleines I, Pham M, Renne T, Stoll G, Nieswandt B. The calcium sensor STIM1 is an essential mediator of arterial thrombosis and ischemic brain infarction. J Exp Med 2008;205:1583–1591.
44. Braun A, Varga-Szabo D, Kleinschnitz C, Pleines I, Bender M, Austinat M, Bosl M, Stoll G, Nieswandt B. Orai1 (CRACM1) is the platelet SOC channel and essential for pathological thrombus formation. Blood 2009;113:2056–2063.
45. Bergmeier W, Oh-Hora M, McCarl CA, Roden RC, Bray PF, Feske S. R93W mutation in Orai1 causes impaired calcium influx in platelets. Blood 2009;113:675–678.
46. Gilio K, van Kruchten R, Braun A, Berna-Erro A, Feijge MA, Stegner D, van der Meijden PE, Kuijpers MJ, Varga-Szabo D, Heemskerk JW, Nieswandt B. Roles of platelet STIM1 and Orai1 in glycoprotein VI- and thrombin-dependent procoagulant activity and thrombus formation. J Biol Chem 2010;285:23629–23638.
47. Harper MT, Poole AW. Store-operated calcium entry and non-capacitative calcium entry have distinct roles in thrombin-induced calcium signalling in human platelets. Cell Calcium 2011;50:351–358.
48. MacKenzie AB, Mahaut-Smith MP, Sage SO. Activation of receptor-operated cation channels via P2X1 not P2T purinoceptors in human platelets. J Biol Chem 1996;271:2879–2881.
49. Hassock SR, Zhu MX, Trost C, Flockerzi V, Authi KS. Expression and role of TRPC proteins in human platelets: evidence that TRPC6 forms the store-independent calcium entry channel. Blood 2002;100:2801–2811.
50. Schedel A, Thornton S, Schloss P, Kluter H, Bugert P. Human platelets express functional alpha7-nicotinic acetylcholine receptors. Arterioscler Thromb Vasc Biol 2011;31:928–934.
51. Reininger AJ. Platelet function under high shear conditions. Hamostaseologie 2009;29:21–22, 24.
52. Gleichman AJ, Spruce LA, Dalmau J, Seeholzer SH, Lynch DR. Anti-NMDA receptor encephalitis antibody binding is dependent on amino acid identity of a small region within the GluN1 amino terminal domain. J Neurosci 2012;32:11082–11094.